Insight into Tyrosine Phosphorylation in v-Fps Using Proton Inventory Techniques[†]

Joseph A. Adams

Department of Chemistry, San Diego State University, San Diego, California 92182-1030

Received March 12, 1996; Revised Manuscript Received June 3, 1996[⊗]

ABSTRACT: The phosphoryl group transfer step in the kinase domain of v-Fps, a nonreceptor tyrosine protein kinase, was analyzed using proton inventory and viscosometric techniques. The latter studies show that two nine-residue peptide substrates for v-Fps, peptides I (EAEAYEAIE) and II (EAEIYEAIE), are in rapid equilibrium with the active site and bind with similar affinities (K_s = 2.2 and 1.7 mM for peptides I and II). While phosphoryl group transfer is the rate-limiting step in k_{cat} for peptide I (5 s^{-1}) at neutral pH, peptide II is converted to product by a kinetic mechanism in which phosphoryl group transfer (45 s^{-1}) and product release (20 s^{-1}) partially control this parameter. Significant solvent isotope effects on k_{cat} ($k_0/k_n \approx 1.6$) are observed for the phosphorylation of both peptides in 95% D_2O. Proton inventories on k_{cat} for peptide I are linear, indicating that the phosphoryl group transfer step is associated with a single proton transfer. Conversely, proton inventories on k_{cat} for peptide II are "bowed" up, consistent with a "virtual" transition state in which phosphoryl group transfer and product release steps partially control this parameter. The lack of solvent isotope effects on $k_{cat}/K_{peptide}$ for both peptides can be explained by an equilibrium isotope effect on substrate binding that offsets the kinetic isotope effect for phosphoryl group transfer. In keeping with this proposal, the K_I for the inhibitor peptide, EAEIFEAIE, is 11 ± 0.80 and 6.5 ± 0.82 mM in 0 and 60% D_2O, respectively. Fitting of the proton inventory plots using modified forms of the Gross−Butler equation provide intrinsic isotope effects of 1.7 and 3.6 for peptides I and II. The combined data are consistent with a mechanism involving either an acid−base catalyst or a conformational change preceding the release of products that is accompanied by the disruption of a single hydrogen donor−acceptor pair.

Protein phosphorylation is central to all signal transduction processes within the cell. The transfer of the γ phosphoryl group from ATP to serine, threonine, and tyrosine targets in proteins and enzymes is catalyzed by a diverse group of catalysts known as protein kinases. This transfer brings about a conformational change in the target that ultimately is linked to specific physiological effects that include changes in carbohydrate and lipid metabolism, DNA transcription, and cell motility and division. Owing to their effects on a host of physiological events, considerable effort has been expended on the structural elucidation of these key enzymes. To date, X-ray crystal structures for the kinase domains of several protein kinases have been solved at high resolution [e.g., DeBont et al. (1993), Hu et al. (1994), Hubbard et al. (1994), Knighton et al. (1991a), Xu et al. (1995), and Zhang et al. (1994)]. Although these enzymes differ greatly in their substrate specificity, they share a number of conserved structural features. In particular, all known protein kinases have a conserved aspartic acid residue positioned near the hydroxyl of the substrate in the active site. In the C-subunit of cAMP-dependent protein kinase (cAPK),[1] Asp-166 is within hydrogen-bonding distance of the hydroxyl of a peptide substrate (Madhusudan et al., 1994). This observation supports the suggestion that Asp-166 in cAPK serves as a general-base catalyst facilitating phosphotransfer.

Despite the structural precedence for general-base catalysis, there is little definitive evidence that a conserved carboxyl side chain in the active site of protein kinases removes the hydroxyl proton of substrates in the chemical transition state. For the serine protein kinases (SPKs), this paucity of evidence may reflect the inability to monitor the chemical step under conditions of steady-state turnover. The rate constant for phosphoryl group transfer in cAPK is 25-fold larger than k_{cat} as determined by pre-steady-state rapid-quench flow methods (Grant & Adams, 1996). A solvent isotope effect (SIE) of 1.6 on k_{cat} for cAPK has been ascribed to the absorption or desorption of one or more protons during the release of products (Yoon & Cook, 1987). The analysis of phosphoryl group transfer in tyrosine protein kinases (TPKs) is simplified owing to the partial expression of the chemical step in k_{cat} (Cole et al., 1994; Wang et al., 1996). A SIE of 1.2 on the phosphorylation of poly(Glu-Tyr) by the TPK Csk (Src C-terminal kinase) has been reported (Cole et al., 1994). These authors argue that this modest isotope effect is reflective of an asymmetric proton transfer in the chemical transition state for this protein kinase. An early proton transfer mechanism for tyrosine phosphorylation by the insulin receptor kinase (Martin et al., 1990) and Csk (Cole et al., 1995) has been discounted owing to the results of kinetic studies with fluorotyrosine-containing peptides. These unnatural peptides are phosphorylated by these two TPKs

[†] This work was supported by the California Metabolic Research Committee and by the American Heart Association, California Affiliate (# 95−274).

[⊗] Abstract published in *Advance ACS Abstracts,* August 1, 1996.

[1] Abbreviations: cAPK, cAMP-dependent protein kinase; Caps, 3-(cyclohexylamino)-1-propanesulfonic acid; Csk, Src C-terminal kinase; GST, glutathione-S-transferase; GST-kin, glutathione-S-transferase linked to the N-terminus of the kinase domain of v-Fps; Mes, 2-(*N*-morpholino)ethanesulfonic acid; MTCN, buffer containing 50 mM Mes, 25 mM Tris, 25 mM Caps, and 50 mM NaCl; SIE, solvent isotope effect; SPK, serine-specific protein kinase; TPK, tyrosine-specific protein kinase; Tris,tris(hydroxymethyl)aminomethane; v-Fps, nonreceptor tyrosine-specific protein kinase of the Fujinami sarcoma virus.

S0006-2960(96)00613-7 CCC: $12.00

with steady-state kinetic parameters that are indistinguishable from their natural analogs despite a pK_a difference of approximately 4 units.

SIEs are observed in chemical reactions involving exchangeable hydrogen when the composition of deuterium in either the ground- or transition-state species is different from the solvent composition. Although SIEs have been observed for TPKs and SPKs, these effects are not clearly understood owing to the absence of detailed proton inventories which describe the nature of the proton transfer(s). In this paper, the application of the proton inventory technique for the study of tyrosine phosphorylation by the nonreceptor TPK v-Fps is described. v-Fps is the prototype for a specific subclass of nonreceptor TPKs that also contains the mammalian Fer TPK and the *Drosophila* Fps homologue (Alcalay et al., 1990; Hao et al., 1989; Katzen et al., 1991; Letwin et al., 1988; Roebroek et al., 1985). We have previously overexpressed and purified large amounts of the kinase domain of v-Fps fused at its N-terminus with glutathione-S-transferase (Gish et al., 1995). This fusion protein, GST-kin, is an ideal model system for the kinetic analysis of nonreceptor TPK catalysis for several reasons. First, GST-kin is autophosphorylated in *Escherichia coli* and shows remarkable catalytic power toward small peptide substrates. Second, GST-kin is not inhibited by phosphorylation either in its kinase domain or in its C-terminal tail so that a fully active species can be studied. Third, the catalytic properties of the kinase domain of GST-kin can be analyzed without intrasteric influences from other domain structures.

The phosphorylation of two nine-residue peptide substrates by the kinase domain of v-Fps was measured in varying amounts of deuterium oxide. Viscosometric and pH-dependent kinetic studies demonstrate that the observed SIEs are not due to changes in buffer or enzyme residue pK_a or to increases in solvent viscosity of D_2O compared to H_2O. The steady-state kinetic data fit well to modified forms of the Gross−Butler equation and indicate that phosphoryl group transfer at the active site of v-Fps is accompanied by a single proton transfer. This SIE can be explained in one of two ways. First, an acid−base catalyst in the active site assists the deprotonation of the tyrosyl hydroxyl in the phosphoryl group transition state. Second, a hydrogen donor−acceptor pair is altered in a conformational change preceding product release.

MATERIALS AND METHODS

Materials. Adenosine 5′-triphosphate (ATP), phosphoenolpyruvate, magnesium chloride, sucrose, glycerol, nicotinamide adenine dinucleotide, reduced (NADH), 2-(*N*-morpholino)ethanesulfonic acid (Mes), tris(hydroxymethyl)-aminomethane (Tris), 3-(cyclohexylamino)-1-propanesulfonic acid (Caps), pyruvate kinase, type II, from rabbit muscle, and lactate dehydrogenase, type II, from bovine heart were purchased from Sigma. Ethylenediaminetetraacetic acid (EDTA) and dithiothreitol (DTT) were purchased from Fisher. Deuterium oxide (D_2O) was purchased from Cambridge Isotopes Laboratories in 1-mL ampoules.

Peptides and Protein. Peptides I and II (Table 1) and the inhibitor peptide, EAEIFEAIE, were synthesized at the USC Microchemical Core Facility using Fmoc chemistry and purified by C-18 reverse-phase HPLC. The concentrations of the peptides were determined by weight. The fusion protein GST-kin, was purified from *E. coli* according to previously published procedures (Gish et al., 1995; Wang et al., 1996) The concentration of the protein was determined by a Bradford assay. The enzyme was stored at −70 °C in a buffer containing 50 mM Tris (pH 7.5), 1 mM EDTA, 150 mM NaCl, 1 mM DTT, and 10% glycerol. The frozen kinase buffer solution was thawed on ice (4 °C) and used immediately for each kinetic study.

Table 1: Steady-State Kinetic Parameters for the Phosphorylation of Peptides by v-Fps[a]

parameter	peptides	
	I (EAEAYEAIE)[b]	II (EAEIYEAIE)[c]
k_{cat} (s^{-1})	6.9 ± 0.10 (high pH) 1.9 ± 0.25 (low pH)	13 ± 0.41
$K_{peptide}$ (mM)	1.9 ± 0.15[d]	0.52 ± 0.032
$k_{cat}/K_{peptide}$ (mM^{-1} s^{-1})	3.8 ± 0.15 (high pH) 1.0 ± 0.45 (low pH)	25 ± 1.7
pK_a (*V*)	6.7 ± 0.07	
pK_a (*V*/*K*)	6.5 ± 0.21	

[a] The kinetic parameters were measured under conditions of saturating ATP (3 mM) and variable peptide in MTCN buffer, 24 °C. [b] These parameters, k_{cat} and $k_{cat}/K_{peptide}$, were determined from fitting the observed values from Figure 1 using eq 3. [c] These parameters represent the average value over the entire pH range (6−9.5). [d] The value reported for $K_{peptide}$ represents the average value over the entire pH range tested.

Kinetic Assay. The enzymatic activity of GST-kin was measured spectrophotometrically using a coupled enzyme assay. This assay couples the production of ADP with the oxidation of NADH using pyruvate kinase and lactate dehydrogenase. In general, varying amounts of peptide I or II were mixed manually with 3 mM ATP, 13 mM $MgCl_2$, and 0.15−0.60 μM GST-kin in a 50 μL (minimum volume) quartz cuvette containing 0.85 mM phosphoenolpyruvate, 0.25 mM NADH, 2 units of lactate dehydrogenase, and 0.5 unit of pyruvate kinase. The total, free concentration of Mg^{2+} was calculated to be 9.4 mM based on the dissociation constants of 0.0143 mM for Mg-ATP, 5 mM for Mg-PEP, and 19.5 mM for Mg-NADH (Martell & Smith, 1977). All reactions were measured in a Beckman DU640 spectrophotometer equipped with a microcuvette holder in a multicomponent buffer containing 50 mM Mes, 25 mM Tris, 25 mM Caps, and 50 mM NaCl (MTCN buffer), in a final volume of 60 μL in either the presence or absence of glycerol or sucrose at 24 °C. Absorbance changes at 340 nm were collected over a time range of 100−200 s. Less than 10% of the substrate peptides were consumed in each initial velocity measurement. Steady-state kinetic parameters were also measured in varying atom fractions (*n*) of deuterium oxide. For high values of *n*, all stock solutions except the enzyme were made up in D_2O. No correction was used for the isotope effect on the pH electrode.

Viscosometric Measurements. The relative solution viscosities (η^{rel}) of buffers containing either glycerol or sucrose were measured relative to a standard buffer of MTCN, pH 7.0, at 24 °C, using an Ostwald viscometer (Shoemaker & Garland, 1962). Each viscosity measurement was carried out using 5.0 mL of buffer containing varying amounts of viscosogen. The amount of time required for each buffer to move through the markings on the viscometer was recorded.

The relative viscosity of each buffer was calculated using

$$\eta^{rel} = \frac{t(\%)}{t}\frac{\rho(\%)}{\rho} \quad (1)$$

where η^{rel} is the relative solvent viscosity, t(%) and t are the transit times for a given viscous buffer and the standard buffer, respectively, and ρ(%) and ρ are the densities of the viscous and standard buffers, respectively. The following relative solvent viscosities were obtained for the buffers (% viscosogen, η^{rel}): 31% glycerol, 2.8; 19% sucrose, 1.7; 25% sucrose, 2.1; 31% sucrose, 2.5. All solvent viscosity measurements were performed in triplicate and did not deviate by more than 2% in value.

Data Analysis. The steady-state kinetic parameters, V_{max} and $K_{peptide}$, were obtained by plotting the initial reaction velocity versus the total substrate concentration according to

$$v = \frac{V_{max}[S]}{K_{peptide} + [S]} \quad (2)$$

where v is the initial reaction velocity, [S] is the total peptide concentration, V_{max} is the maximal reaction velocity, and $K_{peptide}$ is the Michaelis constant. The maximal reaction velocity was converted to k_{cat}, the maximum rate constant, by dividing V_{max} by the total enzyme concentration. Plots of k_{cat} and $k_{cat}/K_{peptide}$ for the phosphorylation of peptide I were fit to

$$y = \frac{C10^{-pH} + C^*10^{-pK_a}}{10^{-pH} + 10^{-pK_a}} \quad (3)$$

where y is the observed value of k_{cat} or $k_{cat}/K_{peptide}$ at a given pH, C^* and C are the maximum and minimum values of these parameters, respectively, and pK_a is the acid dissociation constant. The apparent K_I ($^{app}K_I$) values for the competitive inhibitor peptide, EAEIFEAIE, were measured using a Dixon plot (Dixon, 1953). From the $^{app}K_I$ a true K_I was calculated using the K_m values for the substrate, peptide II, and the relationship $^{app}K_I = K_I (1 + [S]/K_m)$.

RESULTS

pH-Dependent Steady-State Kinetic Studies. The phosphorylation of peptides I and II (Table 1) was monitored as a function of pH (6−9.5) in the multi-component buffer MTCN under conditions of fixed ATP (3 mM) and variable substrate (0.1−16 mM). Plots of v versus substrate concentration were used to determine the steady-state kinetic parameters, k_{cat} and $k_{cat}/K_{peptide}$. Plots of k_{cat} versus pH for peptides I and II are shown in Figure 1. The maximal rate constant for the phosphorylation of peptide II is insensitive to pH over a wide range (6−9.5), while that for peptide I varies with pH. The pH-dependent values for k_{cat} for the phosphorylation of peptide I were fit to eq 3 to obtain the pH-independent values for the parameter and the acid dissociation constant. Plots of $k_{cat}/K_{peptide}$ were also determined for the phosphorylation of both peptides (data not shown). While $k_{cat}/K_{peptide}$ was found to be insensitive to pH for peptide II, this parameter exhibited a similar pH dependence as k_{cat} for peptide I owing to the pH insensitivity

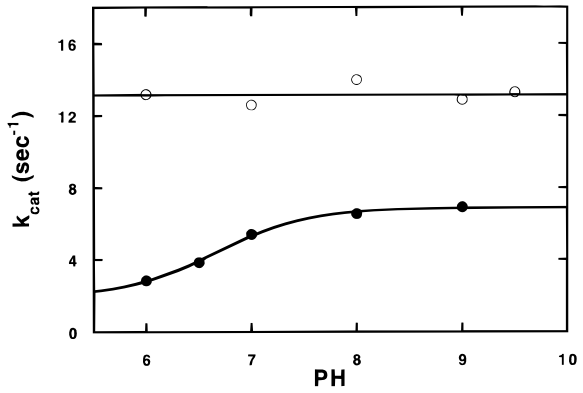

FIGURE 1: pH dependence in k_{cat} for the phosphorylation of peptides I (●) and II (○) under conditions of fixed ATP (3 mM) and variable substrate in MTCN buffer, 24 °C. The curve for peptide I was generated from eq 3.

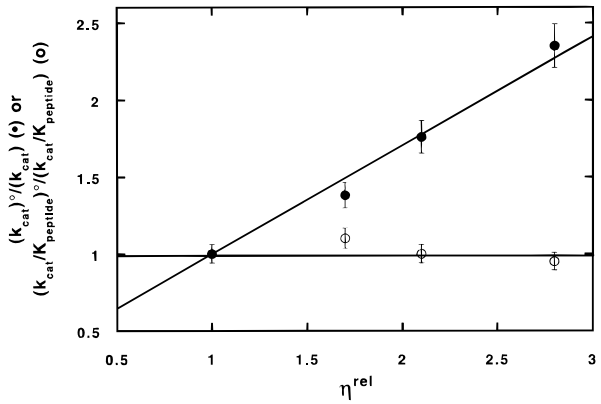

FIGURE 2: Effects of solvent viscosity on the steady-state kinetic parameters, k_{cat} and $k_{cat}/K_{peptide}$, for the phosphorylation of peptide II. $(k_{cat})^0/k_{cat}$ (●) and $(k_{cat}/K_{peptide})^0/(k_{cat}/K_{peptide})$ (○) are the ratios of the observed steady-state kinetic parameters k_{cat} and $k_{cat}/K_{peptide}$ in the absence and presence of viscosogen, respectively, in pH 7 MTCN, 24 °C.

of $K_{peptide}$. The steady-state kinetic parameters are listed in Table 1 for both peptides. The K_m for ATP was measured as a function of pH to ensure that the nucleotide is saturating and that the pH−rate profiles for both peptides are not due to a pH-dependent affinity for this ligand. The K_m for ATP was measured under conditions of fixed peptide II (0.9 mM) at pH values of 6, 7, and 9 and found to be 230 ± 48, 208 ± 16, and 150 ± 50 μM, respectively, so that more than 90% of the total enzyme is in a binary E·ATP form before addition of the substrate. The stability of GST-kin was tested by preequilibrating the enzyme in pH 6, 7, and 9.5 MTCN for varying times before removing small aliquots and assaying for activity in pH 7 MTCN. The activity remained constant for up to 10 min at all pH values, indicating that GST-kin is sufficiently stable over the time course of the assay.

Viscosometric Measurements at Varying pH. The phosphorylation of peptides I and II was measured in the presence of added viscosogens, glycerol and sucrose, at varying pH values in MTCN buffer. The steady-state kinetic parameters, k_{cat} and $k_{cat}/K_{peptide}$, were measured as a function of relative solvent viscosity, η^{rel}, according to previously published methods (Wang et al., 1996). Figure 2 shows a plot of the ratio of the steady-state kinetic parameters for peptide II in the absence and presence of added viscosogen as a function of η^{rel} in pH 7 MTCN. In this plot, $(k_{cat})^0/k_{cat}$ and $(k_{cat}/K_{peptide})^0/(k_{cat}/K_{peptide})$ are the ratios of those parameters in the

Table 2: Viscosometric Parameters for the Phosphorylation of Peptides by v-Fps[a]

parameter	pH	peptides I (EAEAYEAIE)[b]	peptides II (EAEIYEAIE)
$(k_{cat})^{\eta}$	6		0.66 ± 0.061
	7		0.71 ± 0.070
	9	0.15	0.66 ± 0.049
$(k_{cat}/K_{peptide})^{\eta}$	6		-0.050 ± 0.055
	7		-0.038 ± 0.031
	9	−0.0014	0.091 ± 0.10
k_3[c] (s^{-1})	6		38 ± 7.6
	7		45 ± 7.6
	9	6.4	38 ± 6.5
k_4[c] (s^{-1})	6		20 ± 2.6
	7		18 ± 2.4
	9	36	20 ± 2.4

[a] The kinetic parameters were measured under conditions of saturating ATP (3 mM) and variable peptide in MTCN buffer, 24 °C. [b] $(k_{cat})^{\eta}$ and $(k_{cat}/K_{peptide})^{\eta}$ were determined from two viscosity measurements for this peptide. [c] These rate constants were determined from k_{cat} and $(k_{cat})^{\eta}$ according to the following relationships: $k_4 = k_{cat}/(k_{cat})^{\eta}$ and $k_3 = k_{cat}/[1 - (k_{cat})^{\eta}]$ (Wang et al., 1996).

absence (superscript 0) and presence (no superscript) of added viscosogen. The steady-state kinetic parameter k_{cat} varied linearly with η^{rel} and the parameter $k_{cat}/K_{peptide}$ demonstrated little sensitivity to solvent viscosity. The slopes of these lines are designated as $(k_{cat})^{\eta}$ and $(k_{cat}/K_{peptide})^{\eta}$ and are listed in Table 2. This analysis was repeated at pH 6 and 9 for peptide II, and the values of $(k_{cat})^{\eta}$ and $(k_{cat}/K_{peptide})^{\eta}$ were determined and listed in Table 2. The phosphorylation of peptide I was measured in the absence and presence of 31% sucrose ($\eta^{rel} = 2.5$) in pH 9 MTCN and was found to have no effect on $k_{cat}/K_{peptide}$ (3.4 ± 0.32 versus 3.5 ± 0.42 mM^{-1} s^{-1}) and a small effect on k_{cat} (6.9 ± 0.18 versus 5.7 ± 0.21 s^{-1}). From these two viscosity measurements, an estimate of 0.15 for $(k_{cat})^{\eta}$ was determined (Table 2).

Solvent Isotope Effects. For peptide I, the steady-state kinetic parameters, k_{cat} and $k_{cat}/K_{peptide}$, were measured in the absence and presence of 95% D_2O at several pH values. For pH values of 7, 8, and 9 MTCN, SIEs (k_0/k_n) of 1.64 ± 0.049, 1.57 ± 0.047, and 1.63 ± 0.049, respectively, were measured on the maximal rate constant, k_{cat}. For $k_{cat}/K_{peptide}$, no significant SIE was measured over a wide pH range. At pH 7, 8 & 9 MTCN, SIEs of 1.0 ± 0.15, 0.90 ± 0.19, and 0.87 ± 0.16, respectively, were measured. At pH 7 MTCN, a SIE (k_0/k_n) of 1.61 ± 0.08 was measured on k_{cat} for peptide II, while no significant SIE was measured for $k_{cat}/K_{peptide}$ (0.86 ± 0.15). All initial velocity data from which the steady-state kinetic parameters were derived varied linearly with the total enzyme concentration, indicating that D_2O did not influence the ability of the coupling reagents to convert the product ADP to ATP.

The influence of the atom fraction of deuterium on the steady-state kinetic parameters was measured under conditions of saturating ATP (3 mM) for peptides I and II. Figures 3 and 4 display the effects of deuterium atom fraction (n) on k_{cat} for peptides I and II, respectively. The ratio of k_{cat} in the presence and absence of deuterium oxide (k_n/k_0) is plotted against n. For both peptides, $k_{cat}/K_{peptide}$ was found to be insensitive to the atom fraction of deuterium. For example, SIEs of 1.05 ± 0.16, 0.99 ± 0.15, and 0.93 ± 0.16 at $n = 0.25$, 0.60 and 0.90, respectively, were measured for peptide I. Also, SIEs of 0.85 ± 0.18, 1.02 ± 0.17, and 0.95 ± 0.14 at $n = 0.50$, 0.75 and 0.93, respectively, were

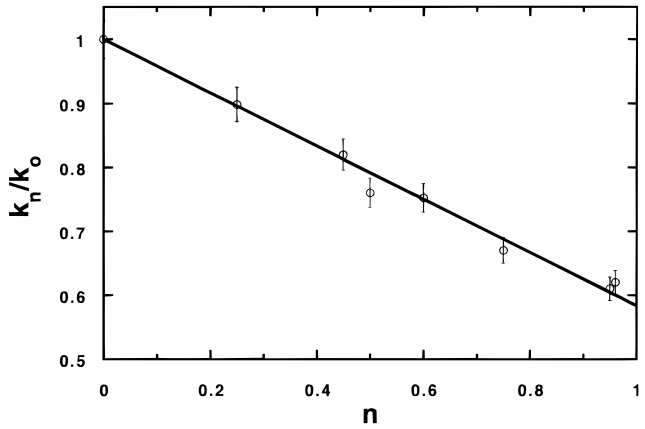

FIGURE 3: Influence of deuterium atom fraction (n) on the steady-state kinetic parameter, k_{cat}, for the phosphorylation of peptide I. The values of k_n/k_0 (○) are the ratios of the observed steady-state kinetic parameter k_{cat} in the presence and absence of varying atom fractions of deuterium (n), respectively, in pH 9 MTCN, 24 °C. The data were fit to eq 6 in the text.

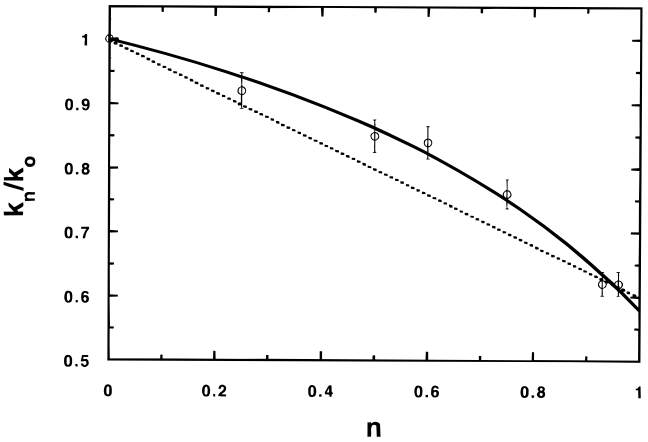

FIGURE 4: Influence of deuterium atom fraction (n) on the steady-state kinetic parameter, k_{cat}, for the phosphorylation of peptide II. The values of k_n/k_0 (○) are the ratios of the observed steady-state kinetic parameter k_{cat} in the presence and absence of varying atom fractions of deuterium (n), respectively, in pH 7 MTCN, 24 °C. The data were fit to eq 7 in the text. The dotted line represents a linear regression fit to the data at $n = 0$, 0.95, and 0.96.

measured for peptide II. To improve the accuracy in the measurements of k_n/k_0, plots of initial velocity versus substrate concentration at any given value of n were performed side-by-side with the water control. Using this procedure, the ratio of k_n/k_0 could be measured with an error of approximately 3%. The standard errors for the measurements of $k_{cat}/K_{peptide}$ were larger than those of k_{cat} for both peptides since the majority of the initial velocity data was collected near or above the $K_{peptide}$ values. The initial reaction velocities were linearly dependent on the enzyme concentration at high values of n, indicating that D_2O did not greatly influence the rate of the coupling enzymes (data not shown).

Influence of Deuterium Oxide on Inhibitor Binding. The dissociation constant (K_I) for the competitive inhibitor EAEIFEAIE was measured in 0 and 60% D_2O under conditions of saturating ATP (3 mM) and fixed concentrations of peptide II (600 μM). The initial velocity of the enzyme reaction was measured as a function of EAEIFEAIE concentration (0−18 mM) and the true K_I was determined using $K_{peptide}$ values of 450 and 300 μM for peptide II in 0 and 60% D_2O, respectively.

DISCUSSION

The application of SIEs for the elucidation of enzyme kinetic mechanisms has been used widely to determine the role of proton transfer in the chemical and nonchemical steps associated with catalysis. Although the observation of a SIE certainly hints at the participation of solvent in the enzyme reaction, a rigorous interpretation of these phenomena is predicated upon detailed proton inventory studies. In this technique, the dependence of a particular rate constant (usually *V* or *V*/*K*) on the atom fraction of solvent deuterium provides invaluable information regarding the number of protons transferred, the participation of conformational changes, and other partially rate-determining events. The theoretical aspects of this approach have been reported thoroughly and many examples have been cited in the literature [for review, Quinn (1987), Schowen and Schowen (1982), and Schowen (1978)].

Although X-ray crystallographic data suggest that a conserved aspartate residue in the active sites of protein kinases may facilitate phosphoryl group transfer by acting as a general-base catalyst, there is little kinetic data to support this hypothesis. Replacement of this aspartate (Asp-166) in cAPK with alanine yields a mutant enzyme that phosphorylates its substrate with a maximum rate constant that is approximately 300-fold lower than that for wild-type (Gibbs & Zoller, 1991). However, mutation of a conserved lysine (Lys-72), the major chelator of the nontransferable α and β phosphates of ATP, has a larger reduction in this kinetic parameter (Gibbs & Zoller, 1991), arguing either that general-base catalysis provides only a small portion of the total catalytic power or that proton abstraction does not occur in the transition state for this protein kinase. SIEs of 1.2 and 1.6 on k_{cat} for Csk (Cole et al., 1994) and cAPK (Yoon & Cook, 1987), examples of TPKs and SPKs, suggest that proton transfer is important for maximum turnover. However, the inability to isolate the phosphoryl group transfer steps for these two examples and to determine the nature of the proton transfer using proton inventory methods undermines a simple interpretation of these effects.

The phosphoryl group transfer step in the nonreceptor TPK v-Fps has been isolated using a viscosometric method and the response of solvent deuterium on the steady-state kinetic parameters, k_{cat} and $k_{cat}/K_{peptide}$, has been measured. By applying this dual solvent perturbation technique to the phosphorylation of a good and poor substrate for this enzyme, it is demonstrated that the phosphoryl group transfer step is accompanied by a single proton transfer. The data are consistent with one of two possible catalytic mechanisms—a general acid−base catalytic mechanism or a mechanism involving a deuterium-sensitive, conformational change preceding product release. In order to interpret the effects of deuterium oxide on the phosphorylation kinetics catalyzed by v-Fps, though, two issues must be addressed. First, it is important to know which individual step or steps in the kinetic mechanism limit the steady-state kinetic parameters. Second, it is important to know whether equilibrium effects on acid dissociation constants provide a source for an observed SIE. The following two sections address these issues.

Rate-Determining Step(s) for Tyrosine Phosphorylation. It has been demonstrated previously that k_{cat} is partially limited by both phosphoryl group transfer and a diffusion-controlled step, namely, product release, for the kinase domain of v-Fps (Wang et al., 1996). These studies were performed with good substrates for v-Fps in a pH 7 buffer containing 100 mM Mops. To further characterize this kinetic pathway, the effects of pH on the phosphorylation of peptides were studied in a multicomponent buffer system. These peptides (Table 1) were selected on the basis of differing selectivities for v-Fps. At pH 7, the apparent second-order rate constant, $k_{cat}/K_{peptide}$, for peptide II is approximately 8-fold larger than that for peptide I (Table 1). These peptides differ at only one amino acid residue, namely the P − 1 position.[2] The poorer phosphorylation rates for peptide I compared to peptide II are consistent with the predictions of a random peptide library study on v-Fps (Songyang et al., 1995). For peptide II, none of the steady-state kinetic parameters varied with pH, while those for peptide I showed a distinct sensitivity to pH (Table 1 and Figure 1).

Scheme 1

$$\text{E·ATP} + \text{S} \underset{k_{-2}}{\overset{k_2}{\rightleftharpoons}} \text{E·ATP·S} \xrightarrow{k_3} \text{E·ADP·P} \xrightarrow{k_4}$$

The phosphorylation kinetics for peptides I and II were measured as a function of solvent viscosity to gain insight into the kinetic mechanism of v-Fps. The influence of viscosity on the steady-state kinetic parameters was interpreted according to a three-step mechanism as shown in Scheme 1. In this mechanism, substrate binds the E•ATP binary complex by the association and dissociation rate constants, k_2 and k_{-2}, respectively. The catalytic step, k_3, describes the favorable, unimolecular transfer of the γ phosphoryl group of ATP to the hydroxyl of tyrosine. The irreversibility of this step is supported by measurements on k_{cat} in the forward and reverse reactions catalyzed by c-Src, a related nonreceptor TPK (Boerner et al., 1995). The final step in Scheme 1 (k_4) describes the net unimolecular rate constant for the release of both products. By inserting viscosity dependencies on k_2, k_{-2}, and k_4 into the expressions for k_{cat} and $k_{cat}/K_{peptide}$, linear functions of the ratios of k_{cat} and $k_{cat}/K_{peptide}$ in the absence and presence of viscosogen versus η^{rel} are obtained. Equations 4 and 5 represent the slopes of these equations for both steady-state kinetic parameters:

$$(k_{cat})^{\eta} = \frac{k_3}{k_3 + k_4} \tag{4}$$

$$(k_{cat}/K_{peptide})^{\eta} = \frac{k_3}{k_{-2} + k_3} \tag{5}$$

where $(k_{cat})^{\eta}$ and $(k_{cat}/K_{peptide})^{\eta}$ are the slopes of $(k_{cat})^0/k_{cat}$ and $(k_{cat}/K_{peptide})^0/(k_{cat}/K_{peptide})$ versus η^{rel}, respectively. Steady-state kinetic parameters that are diffusion-controlled will be maximally sensitive to solvent viscosity and exhibit slopes close to 1 for the expressions in eqs 4 and 5. In these cases, only a lower limit can be placed on k_3, and k_{cat} and $k_{cat}/K_{peptide}$ are limited by k_4 and k_2, respectively. Conversely,

[2] For peptides I and II, the site of tyrosine phosphorylation is the P-site. All positions N-terminal to the tyrosine are designated P − 1, P − 2, P − 3, etc., and all positions C-terminal are designated P + 1, P + 2, P + 3, etc.

when the steady-state kinetic parameters are insensitive to solvent viscosity and the values of eqs 4 and 5 are close to 0, only lower limits can be placed on k_{-2} and k_4, and k_{cat} and $k_{cat}/K_{peptide}$ are limited by k_3 and k_3k_2/k_{-2}, respectively. For intermediate values of both $(k_{cat})^{\eta}$ and $(k_{cat}/K_{peptide})^{\eta}$ (i.e.; slopes between 0 and 1), all rate constants in Scheme 1 can be determined.

The influence of solvent viscosity on the phosphorylation of both peptides was measured in MTCN buffer at several pH values to determine whether pH alters any of the individual steps in Scheme 1. For peptide II, $(k_{cat})^{\eta}$ did not vary over the pH range of 6−9.5, indicating that no changes in k_3, k_4, or K_s occur. These data also indicate that peptide II is phosphorylated by a kinetic mechanism in which the substrate is in rapid equilibrium with the E·ATP binary complex (i.e., $k_{-2} \gg k_3$) and phosphoryl group transfer and product release partially control maximum turnover over all pH values. For peptide I, no large effect of solvent viscosity on either k_{cat} or $k_{cat}/K_{peptide}$ was measured at the pH optimum (pH 9), indicating that the substrate is in rapid equilibrium and the phosphoryl group transfer step is rate-determining for k_{cat} (i.e., $k_4 > k_3$). On the basis of these observations, it is presumed that the pH sensitivity of k_{cat} and $k_{cat}/K_{peptide}$ for peptide I is due to a small pH dependence in k_3. The lack of a pH dependence on $K_{peptide}$ or on the K_m for ATP supports the assumption that substrate association and presumably product dissociation are pH-insensitive and not rate-determining for peptide I at pH values less than 9. This assumption is further supported by the observation that the net release rate of products for the phosphorylation of peptide II is pH-insensitive.

From the viscosity data, the true affinities of the two substrates ($K_s = k_{-2}/k_2$) can be determined from $K_{peptide}$ and $(k_{cat})^{\eta}$ according to the relationship $K_s = K_{peptide}/[1 - (k_{cat})^{\eta}]$. This relationship stems from the observation that the substrates are in rapid equilibrium and $(k_{cat})^{\eta}$ is less than unity (Wang et al., 1996). Values of 2.2 and 1.7 mM were determined from this relationship for peptides I and II. A striking feature of this kinetic mechanism (Scheme 1) is that $K_{peptide}$ is not equal to K_s and that the enhanced selectivity of peptide II compared to peptide I is not due to improved binding of this peptide but rather to an enhanced rate of phosphoryl group transfer (Table 2).

Influence of pH on SIEs. Deuterium oxide can have measurable effects on the acid dissociation constants of key enzyme residues important for catalysis and on those of the buffer components. Although these isotope effects are often compensated by the standard isotope effect on the pH electrode (Fersht, 1985), it is necessary to measure SIEs on kinetic parameters at a number of pH values. This study controls for any large SIEs that may arise from alterations in acid dissociation constants rather than from real transition-state phenomena. Since no pH dependence in any of the steps in Scheme 1 was detected for peptide II using viscosometric methods, this control is not required. However, since k_{cat} and $k_{cat}/K_{peptide}$ for peptide I varies with pH (Figure 1 and Table 2), SIEs were measured over several pH values. No change in the observed SIE was detected over a pH range from 7 to 9. Consequently, the observed effect is not due to an equilibrium isotope effect on a catalytic residue or on buffer pK_a. This is indeed a fortuitous outcome that streamlines the interpretation of SIEs on enzyme catalysis. Frequently, the pH response of the steady-state kinetic parameters is altered by the substitution of deuterium oxide. Under these circumstances the observed SIEs must be corrected by the observed change in pK_a (Quinn, 1987).

Finally, the observed SIEs are not due to the larger intrinsic viscosity of deuterium oxide compared to water for two reasons. First, the observed SIEs of 1.6 at 95% D_2O for both peptides are much larger than the predicted influence of the isotope on the solvent viscosity. Since D_2O is 20% more viscous than water at room temperature and the diffusion-controlled step (k_4) in k_{cat} is partially rate-limiting for peptide II (Table 2), the effects of increased viscosity would only account for 14% rather than the observed 70% change in turnover rate. Second, k_{cat} is little affected by solvent viscosity for peptide I yet a large SIE is observed for this substrate.

Proton Inventory Studies. The viscosometric data in Table 2 define the rate-determining steps in the steady-state kinetic parameters, and the pH-dependent isotope studies demonstrate that no equilibrium effects influence the kinetic SIEs on k_{cat}. With this as a foundation, proton inventory methods can now be applied and interpreted. While both peptides exhibit SIEs of approximately 1.6 on k_{cat} at 95% D_2O, the responses of this parameter to the atom fraction of solvent deuterium are strikingly different. For peptide I, a linear dependence of k_n/k_0 on deuterium atom fraction is observed, while a curved dependence is observed for peptide II. These data were interpreted according to modified forms of the Gross−Butler equation which relate the rate constant of a reaction to atom fraction by a fractionation term (ϕ) for the heavy isotope composition in either the ground- or transition-state complexes. For peptide I, the linear response of k_{cat} is most consistent with a single proton transfer governing the transition state for this parameter. The data were fit to

$$k_n/k_0 = 1 + n(\phi_3 - 1) \qquad (6)$$

where ϕ_3 is the transition-state fractionation factor for k_3 and n is the deuterium atom fraction. This linear relationship fits well to the experimental data in Figure 3. From this fit a fractionation factor (ϕ_3) of 0.59 ± 0.013 and an intrinsic SIE of 1.7 ($1/\phi_3$) can be determined. Since the rate-determining step in k_{cat} for peptide I is k_3, based on viscosity studies (Table 2), the fractionation factor and SIE obtained from the fitting of eq 6 to the data in Figure 3 correspond to a single step in the kinetic mechanism of Scheme 1, namely, phosphoryl group transfer.

The proton inventory curve for peptide II is more complex than that for peptide I. The curvilinear plot in Figure 4 has been observed previously for other enzymes and has been interpreted as originating from a "virtual" transition state (Quinn, 1987). In this special case, the plot is "bowed" up owing to a kinetic mechanism in which a deuterium-sensitive step and deuterium-insensitive step partially limit k_{cat}. The data in Figure 4 were fit to a modified form of eq 6 in which a second, partially rate-determining step has been inserted. This new equation is shown below:

$$k_n/k_0 = \frac{1 + n(\phi_3 - 1)}{1 + f_3 n(\phi_3 - 1)} \qquad (7)$$

where $f_3 = k_3/(k_3 + k_4)$ and ϕ_3 has the same definition as in eq 6. Note that f_3 has the identical mathematical form as $(k_{cat})^{\eta}$ in eq 4. The data fit well to eq 7 and provide values

of 0.72 ± 0.046 and 0.28 ± 0.043 for f_3 and ϕ_3, respectively. This places an intrinsic SIE of 3.6 on k_3 for peptide II. The value of f_3 provides a quantitative measure of the contribution of k_3 toward maximum turnover. The similar values of f_3 and $(k_{cat})^{\eta}$ (Table 2) support the interpretation of the solvent isotope studies and provide a compelling argument for this interpretation of the kinetic data.

Since both peptides are in rapid exchange with the enzyme, the phosphoryl group transfer step should be expressed in the equation for $k_{cat}/K_{peptide}$ (i.e., $k_{cat}/K_{peptide} = k_3/K_s$). As a result, a SIE is expected in this kinetic parameter for both peptides. Surprisingly, no effect is observed. Although this inconsistency could be explained by a favorable, deuterium-insensitive step preceding phosphoryl group transfer, the inhibition data suggest another solution. The dissociation constant for the competitive inhibitor EAEIFEAIE was found to be lower in 60% D_2O compared to the water control by approximately 1.7-fold. Given a predicted SIE of approximately 2 for k_3 at 60% D_2O for peptide II,[3] the equilibrium isotope effect on the binding of the substrate offsets this so that no SIE is observed for $k_{cat}/K_{peptide}$. This effect on substrate binding is not unique for v-Fps but rather has been observed for another TPK. Studies on Csk indicate that this equilibrium effect may also be present for the phosphorylation of poly(Glu-Tyr). A SIE is observed on the K_m [$K_m(H)/K_m(D) \approx 2.8$] for this substrate, corroborating the inhibitor results presented in this paper (Cole et al., 1994). These observations make the quantitative analysis of $k_{cat}/K_{peptide}$ difficult owing to the inability to isolate a single deuterium-sensitive step in this parameter.

Catalysis and Proton Transfer. The data presented herein establish firmly the role of solvent in the phosphorylation of substrates by the nonreceptor TPK v-Fps. The data from both viscosity and solvent isotope studies are consistent and confirm that the kinase domain of v-Fps phosphorylates good substrates by a kinetic mechanism in which phosphoryl group transfer and product release partially limit maximum turnover. In contrast, the phosphorylation of poor substrates occurs by a similar kinetic mechanism that differs in only one step, namely, k_3. The 8-fold difference in $k_{cat}/K_{peptide}$ for peptides I and II can be explained by changes in k_3 rather than by changes in K_s (Scheme 1 and Table 2). These data suggest that the P − 1 position is critical for sustaining rapid phosphoryl group transfer and not important for substrate binding. Further studies of peptide analogs will define the roles of other key positions for binding and catalysis for this TPK.

The observation of large kinetic SIEs on the phosphoryl group transfer steps for peptides I and II suggests that solvent plays an important role in the chemical event in the enzyme's active site. However, the participation of a single proton in this step can have one of two origins. First, the SIE may arise from the ionization of an acid−base catalyst in the active site. Second, the effect may arise from a conformational change preceding the release of product. This latter explanation implies that a single hydrogen donor−acceptor pair is disrupted in this conformational event. Furthermore, this structural change may precede, follow, or be concerted with the phosphoryl group transfer step. This fine distinction is indeterminate, at this point, since the viscosity method only provides direct information on the product release step(s). The former interpretation invokes the participation of an amino acid side chain in the active site that helps ionize the tyrosyl hydroxyl. Indeed, there is substantial structural evidence from the X-ray analysis of cAPK that a conserved aspartate (Asp-166 in cAPK; Asp-1043 in v-Fps) is within hydrogen-bonding distance of the hydroxyl and, therefore, may serve as a general-base catalyst (Madhusudan et al., 1994).

The possibility that Asp-1043 performs the role of a general-base catalyst and is the source of this SIE is consistent with the early predictions from the x-ray structure of cAPK (Knighton et al., 1991a,b). However, the lack of a pH dependence of k_3 in Scheme 1 appears to weaken this possibility. Two explanations can be offered to explain these observations. First, the pK_a of this residue may be much higher than its solvent pK_a owing to neighboring effects in the active site. This is not an uncommon feature of enzyme catalysis. For example, the active-site pK_a of the proton donor, Asp-26, in a mutant form of dihydrofolate reductase is more than 4 units higher than its solvent value (Adams et al., 1989). Second, the active-site pK_a for Asp-1043 may be low but may exhibit a much larger value in the transition state for phosphoryl group transfer. Transition state pK_as may be significantly different than their solvent values. This difference has been used to account for the ability of weak catalytic bases to abstract highly basic protons through the formation of low-barrier hydrogen bonds (Cleland & Kreevoy, 1994). Since no rate enhancement is observed at pH 9 (Table 2), a pH at which approximately 20% of the tyrosyl side chain is ionized, it is presumed that this putative catalytic base has sufficient basicity to abstract the hydroxyl proton over all pH values tested and that the pK_as of Asp-1043 and the substrate tyrosine are matched in the transition state. The possibility that the hydroxyls of the tyrosine peptides may be ionized in the active site of two TPK, Csk (Cole et al., 1995) and the insulin receptor (Martin et al., 1990), in a preprotonation mechanism has been discounted on the basis of studies of fluorotyrosine substrate analogs. The inability to correlate the pK_a of the phenolic acceptor with catalysis in these two examples suggests that the hydroxyl proton is too basic to be abstracted in the ground-state complex. It is presumed that this is also true for v-Fps and its substrates.

A small pH dependence in k_{cat} for peptide I (Table 1) has been ascribed to a small pH dependence in k_3 on the basis of viscosity measurements (Table 2). However, it is unlikely that this pH sensitivity is due to the ionization of an acid−base catalyst for two reasons. First, this ionization does not affect the phosphoryl group transfer step for peptide II despite a larger intrinsic SIE for this peptide compared to peptide I. Second, the difference in the rate of phosphoryl group transfer at low and high pH for peptide I is less than 4-fold (Table 1), suggesting that the general-base catalyst provides less than 1 kcal/mol of transition-state stabilization energy. In contrast, mutation of Asp-1043 in v-Fps to glutamate leads to an inactive kinase (Moran et al., 1988), suggesting that proton abstraction contributes far more than this amount toward lowering the transition-state energy barrier. Since the effects of pH on the chemical event are small, it is likely that the observed pK_a of 6.7 (Table 1) is due to the ionization of a residue distal from the site of phosphoryl group transfer.

[3] Since k_3 is linearly dependent on the atom fraction of deuterium and an intrinsic SIE ($1/\phi_3$) of 3.6 is measured for the phosphotransfer step, the observed value of k_3 at any given value of n can be estimated from the relationship, $k_n/k_0 = 1 - n + n\phi_3$.

The potential role of Asp-1043 as a general-base catalyst raises an interesting question regarding the nature of phosphoryl group transfer in SPKs and TPKs. Do both classes of protein kinases facilitate phosphotransfer by general-base mechanisms? Although an aspartate residue is conserved in all protein kinases, it may not serve the same function in both enzyme groups. The data in this paper suggest that general-base catalysis is a possible element for phosphoryl group transfer in TPKs. The results from mutagenesis studies on cAPK and Csk argue that the mechanisms may be identical. Removal of the conserved aspartate residue in cAPK (Gibbs & Zoller, 1991) and Csk (Cole et al., 1995) leads to reductions in k_{cat} of 300- and 10 000-fold, respectively. By correcting for the true rate of phosphoryl group transfer in the former enzyme [$k_3 \approx 25k_{cat}$ (Grant & Adams, 1996)], both mutations have similar effects on the chemical step, inferring that the conserved residue performs identical tasks for both enzymes. We are currently testing this hypothesis on cAPK using rapid-quench flow techniques and solvent isotope studies.

REFERENCES

Adams, J. A., Johnson, K., Matthews, R., & Benkovic, S. J. (1989) *Biochemistry 28*, 6611−6618.

Alcalay, M., Antolini, F., Van de Ven, W. J., Lanfrancone, L., Grigani, F., & Pelicci, P. G. (1990) *Oncogene 5*, 267−275.

Boerner, R. J., Barker, S. C., & Knight, W. B. (1995) *Biochemistry 34*, 16419−16423.

Cleland, W. W., & Kreevoy, M. M. (1994) *Science 264*, 1887−1890.

Cole, P. A., Burn, P., Takacs, B., & Walsh, C. T. (1994) *J. Biol. Chem. 269*, 30880−30887.

Cole, P. A., Grace, M. R., Phillips, R. S., Burn, P., & Walsh, C. T. (1995) *J. Biol. Chem. 270*, 22105−22108.

DeBont, H. L., Rosenblatt, J., Jancarik, J., Jones, H. D., Morgan, D. O., & Kim, S. H. (1993) *Nature 363*, 595−602.

Dixon, M. (1953) *Biochem. J. 55*, 170.

Gibbs, C. S., & Zoller, M. J. (1991) *J. Biol. Chem. 266*, 8923−8931.

Gish, G., McGlone, M. L., Pawson, T., & Adams, J. A. (1995) *Protein Eng. 8*, 609−614.

Grant, B., & Adams, J. A. (1996) *Biochemistry 35*, 2022−2029.

Hao, Q., Heisterkamp, N., & Groffen, J. (1989) *Mol. Cell. Biol. 9*, 1587−1593.

Hu, S. H., Parker, M. W., Lei, J. Y., Wilce, M. C., Benian, G. M., & Kemp, B. E. (1994) *Nature 369*, 581−584.

Hubbard, S. R., Wei, L., Ellis, L., & Hendrickson, W. A. (1994) *Nature 372*, 746−754.

Katzen, A. L., Montarras, D., Jackson, J., Paulson, R. F., Kornberg, T., & Bishop, J. M. (1991) *Mol. Cell. Biol. 11*, 226−239.

Knighton, D. R., Zheng, J., Ten Eyck, L. F., Ashford, V. A., Xuong, N.-h., Taylor, S. S., & Sowadski, J. M. (1991a) *Science 253*, 407−414.

Knighton, D. R., Zheng, J., Ten Eyck, L. F., Xuong, N.-h., Taylor, S. S., & Sowadski, J. M. (1991b) *Science 253*, 414−420.

Letwin, K., Yee, S., & Pawson, T. (1988) *Oncogene 3*, 621−627.

Madhusudan, Trafny, E. A., Xuong, N.-h., Adams, J. A., Ten Eyck, L. F., Taylor, S. S., & Sowadski, J. M. (1994) *Protein Sci. 3*, 176−187.

Martell, A. E., & Smith, R. M. (1977) *Critical Stability Constants*, Vol. 3, Plenum, New York.

Martin, B. L., Wu, D., Jakes, S., & Graves, D. J. (1990) *J. Biol. Chem. 265*, 7108−7111.

Moran, M., Koch, A., Sadowski, I., & Pawson, T. (1988) *Oncogene 3*, 665−672.

Quinn, D. M. (1987) *Chem. Rev. 87*, 955−979.

Roebroek, A. J. M., Schalken, J. A., Verbeek, J. S., Van den Ouweland, A. M. W., Onnekink, C., Bloemers, H. P. J., & Van de Ven, W. J. M. (1985) *EMBO J. 4*, 2897−2903.

Schowen, K. B. J. (1978) in *Transition States of Biochemical Processes* (Gandour, R. D., & Schowen, R. L., Eds.) pp 225−283, Plenum Press, New York.

Schowen, K. B., & Schowen, R. L. (1982) *Methods Enzymol. 87*, 551−605.

Shoemaker, D. P., & Garland, C. W. (1962) *Experiments in Physical Chemistry*, 2nd ed., McGraw-Hill, New York.

Songyang, Z., Carraway, K. L., Eck, M. J., Feldman, R. A., Mohammadl, M., Schlessinger, J., Hubbard, S. R., Smith, D. P., Eng, C., Lorenzo, M. J., Ponder, B. A. J., Mayer, B. J., & Cantley, L. C. (1995) *Nature 373*, 536−539.

Wang, C., Lee, T. R., Lawrence, D. S., & Adams, J. A. (1996) *Biochemistry 35*, 1533−1539.

Xu, R.-M., Carmel, G., Sweet, R. M., Kuret, J., & Cheng, X. (1995) *EMBO J. 14*, 1015−1023.

Yoon, M.-Y., & Cook, P. F. (1987) *Biochemistry 26*, 4118−4125.

Zhang, F., Strand, A., Robbins, D., Cobbs, M. H., & Goldsmith, E. J. (1994) *Nature 367*, 704−711.

BI960613H